TRANSPORT CALCULATIONS FOR LIGHT SCATTERING IN BLOOD

G. D. PEDERSEN, N. J. McCORMICK, *and* L. O. REYNOLDS

From the Department of Nuclear Engineering and the Center for Bioengineering, University of Washington, Seattle, Washington 98195. Mr. Pedersen's present address is Bechtel Corporation, San Francisco, California 94119.

ABSTRACT In vivo measurement of the oxygen saturation levels in blood may be obtained from relative amounts of backscattered monochromatic light at two different wavelengths, as measured with a fiber-optic catheter oximeter. Because of the short mean free path length of light in blood, the backscattering can be well approximated by a previously-derived, one-wavelength transport theory solution for the half-space searchlight problem. This solution, unlike simple diffusion approximations, has the advantage that the boundary condition describing illumination of a localized area of blood by a monodirectional light beam can be rigorously satisfied. Sample calculations using the solution are compared with experimental values of the reflectance of blood.

INTRODUCTION

Increased interest, in recent years, in the application of fiber optics to the field of bioinstrumentation has lead to the development of a fiber-optic oximeter for the measurement of oxygen saturation in human blood in vivo. Polanyi (1) along with Enson et al. (2) were among the first to use fiber-optic oximeters for in vivo studies. Such an oximeter, which consists of a cylindrical bundle of transmitting and receiving fiber optics mounted in a catheter, can illuminate blood by conveying light through some of the fibers to the tip, or distal end, of the catheter. Light is scattered and absorbed by the blood in the immediate vicinity of the tip and a portion is reflected back onto the distal end from red blood cells in intracardiac and other intravascular sites (3–5). There it is picked up by the second set of optical fibers and transmitted back to a photosensitive receiver at the proximal end.

Light is transmitted at the wavelengths of about 0.935 μ (or 0.805 μ) and 0.685 μ (or 0.66 μ) in order to take optimum advantage of differences in the absorption characteristics of oxygenated and deoxygenated blood. The oxygen saturation level is related to a ratio of the reflectance at the two wavelengths (1).

Early analytical studies of the propagation of light in blood were performed by Anderson and Sekelj (6) who used a special case of Twersky's multiple wave scattering theory (7) to explain experimental data available on the scattering and absorption of light in whole human blood. At normal hematocrit values, however, blood is sufficiently dense that such an application of the theory is poor.

A more accurate mathematical model was introduced by Longini and Zdrojkowski (8) who solved for the optical transmittance and reflection using equations from diffusion theory. The diffusion theory approach, or a special case of it, was also used by Zdrojkowski and Pisharoty (9), Johnson (10), Cohen and Longini (11), and Janssen (12), in which either a Lambertian or a monodirectional distribution of incident intensity and isotropic scattering was assumed. The major deficiencies of the usual diffusion theory approach for transport in blood are: (*a*) angle-dependent boundary conditions, such as are needed for a monodirectional beam incident on a surface of blood, cannot be properly taken into account, and (*b*) only the two lowest angular moments of the angle-dependent intensity (the total intensity and the current) may be calculated.

By far the most important of these limitations is the first, especially since we may desire only the total reflectance from the blood and not an angle-dependent reflectance. There are two ways to correctly impose such boundary conditions: either perform angle-dependent transport calculations or use diffusion theory with a spatially-distributed source inside the blood arising from the first-collided distribution.

It is the purpose of this paper to eliminate such a deficiency by making angle-dependent calculations which better describe the propagation of light through blood. It is hoped that this presentation ultimately will enable fiber-optic catheter oximeters to be better designed. The utility of the procedure depends, in turn, upon the accuracy of physical parameters available; experimental measurements of these parameters are outside the scope of this work.

COMPUTATIONAL PROCEDURE

The numerical solution utilized here solves the one-wavelength transport theory expressions for the reflection from a semi-infinite medium, illuminated by an incident beam having a small cross-sectional area. Such a geometry is reasonable based upon the short mean free path length of red and infrared light in blood compared with the diameter of an artery or vein. The theoretical developments were carried out by Rybicki (13), who solved the three-dimensional searchlight problem in the semi-infinite and slab geometries.

The sourceless, time-independent, one-wavelength transport equation in three dimensions for isotropic scattering is

$$\Omega \cdot \nabla \Phi(p, \Omega) + \sigma \Phi(p, \Omega) = \frac{w\sigma}{4\pi} \int_{4\pi} \Phi(p, \Omega') d\Omega', \qquad (1)$$

where $\Phi(p, \Omega)$ is the angular intensity at point p and wavelength λ in the direction defined by the unit vector Ω (the symbol λ is suppressed here and henceforth); σ is the macroscopic interaction cross section in square millimeters (the density multiplied by the microscopic cross section); w is the ratio of the scattering to total cross sections. Eq. 1 describes the radiation transport process for unpolarized light and is comprised

of three terms accounting for streaming, losses by interactions, and gains by scattering processes.

At first glance it would appear this equation is unsuitable for treating the highly anisotropic (small angle) scattering of light in blood. Because the light is relatively nonabsorbing, this limitation can be largely corrected in calculations by replacing σ by the transport cross section σ_* (14),

$$\sigma_* = \sigma - \bar{\mu}\sigma_s, \tag{2}$$

as used in a diffusion theory analysis. Here σ_s is the macroscopic scattering cross section and $\bar{\mu}$ is the average cosine of the scattering angle, given in terms of the differential scattering function $f(\mu)$ by

$$\bar{\mu} = 2\pi \int_{-1}^{1} f(\mu)\mu \, d\mu. \tag{3}$$

Although the analysis would be improved by use of detailed angle-dependent scattering cross sections, such data is presently limited (9, 11, 15) and hence Eqs. 2 and 3 form a good way in which to treat a one-parameter ($\bar{\mu}$) scattering model.

By assuming azimuthal symmetry, Eq. 1 can be written in the form

$$\mu \frac{\partial}{\partial z}\Phi(z,r,\mu) + \nu \frac{\partial}{\partial r}\Phi(z,r,\mu) + \sigma_*\Phi(z,r,\mu) = \frac{1}{2} w\sigma_* \int_{-1}^{1} \Phi(z,r,\mu')\, d\mu', \tag{4}$$

where the vector p has been decomposed into its depth-component, z, and a radial-component r, lying in the $x - y$ plane. Similarly, Ω has been decomposed into its z-component ($\mu = \cos\theta, 0 \le \theta \le \pi$) and the ν-component ($\nu = (1 - \mu^2)^{1/2}$) lying in the $x - y$ plane.

The boundary condition for the intensity incident at $z = 0$ and $r = 0$ is

$$\Phi(0,r,\mu) = F(2\pi\mu)^{-1}\delta(r)\delta(\mu - \mu_0), \qquad \mu > 0, \tag{5}$$

where F is a constant to denote the magnitude of the flux from the incoming beam. A second condition is that the intensity tends to vanish as z becomes large.

The solution of Eq. 4, subject to the two conditions, follows by taking Fourier transforms (13). The generalization of Chandrasekhar's S-function (16), in terms of the inverse Fourier transform of complex H-functions, is (13)

$$S(\mu_0,\mu;r) = (2\pi)^{-2} \int_{-\infty}^{\infty} dk e^{-ikr} \frac{wH(\rho,k)H(\rho_0,k)}{(1/\rho) + (1/\rho_0)}, \qquad \mu,\mu_0 > 0, \tag{6}$$

where ρ is a complex cosine defined by

$$\rho = \mu(1 - ik\nu)^{-1} \tag{7}$$

and k is the Fourier transform variable. Here S is the scattering function at r and μ

for diffuse reflection from a semi-infinite, plane-parallel medium subjected to an azimuthally-symmetric illumination located at μ_0. The distance r separating the transmitting and receiving points is now measured in units of the transport mean free path (mfp),

$$\lambda_{tr} = 1/\sigma_s. \tag{8}$$

The H-functions satisfy the nonlinear integral equation (13, 16)

$$H(\mu, k) = 1 + \frac{w\mu}{2} \int_0^{(1+k^2)^{-1/2}} \frac{d\mu'}{(\mu + \mu')(1 - k^2\mu'^2)^{1/2}} H(\mu, k)H(\mu', k). \tag{9}$$

Once Eq. 6 has been solved for the S-function, the outgoing current can easily be found from

$$J_{OUT}(r) = \frac{1}{2} \int_0^1 S(\mu_0, \mu; r)d\mu, \qquad \mu_0 > 0. \tag{10}$$

The first step in the numerical solution to the searchlight problem was the computation of the complex H-function, $H(\rho, k)$. A computer code was written to accomplish this by means of the kernel approximation method (13, 17). The approximate equation for the H-function from this method is

$$H(\rho, k) = \prod_{i=1}^{N} \frac{\rho^{-1} + [1/\mu_i^2 + k^2]^{1/2}}{\rho^{-1} + [\gamma_i^2 + k^2]^{1/2}}, \tag{11}$$

where the γ_i^2 are the roots of the characteristic equation

$$1 = \frac{1}{2} w \sum_{i=1}^{N} \frac{\omega_i}{1 - \mu_i^2\gamma_i^2}. \tag{12}$$

The ω_i and μ_i in Eqs. 11 and 12 are the half-range Gaussian weights and nodes, respectively, while $2N$ is the order of the Gauss quadrature.

After calculating the complex H-functions from Eq. 9, the Cooley-Tukey algorithm (18), was used to solve for the S-function from Eq. 6, and then Eq. 10 was evaluated for the outgoing current. Convergence with the algorithm was assured by comparing the reflected current results using 256, 512, and 1,024 point calculations, which indicate an accuracy of three significant figures could be achieved by utilizing 512 point calculations in this study.

NUMERICAL RESULTS

In Fig. 1 the S-function obtained from Eq. 6 is plotted as a function of μ for several values of r for the case of a normally incident beam, $\mu_0 = 1$, using the data given in the Appendix. The distance r is the separation between a single transmitting and a single receiving point. In actual practice, however, the fiberoptics for transmitting

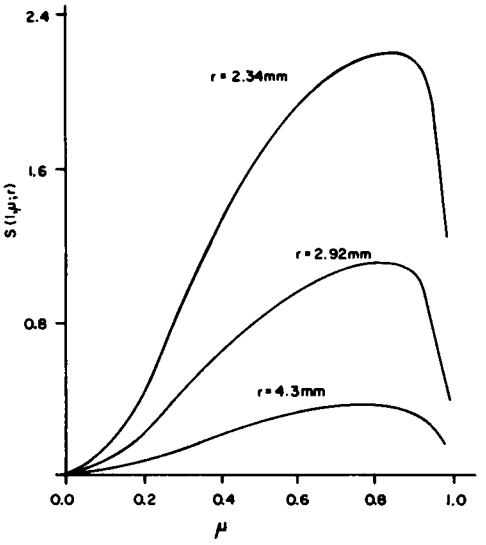

FIGURE 1

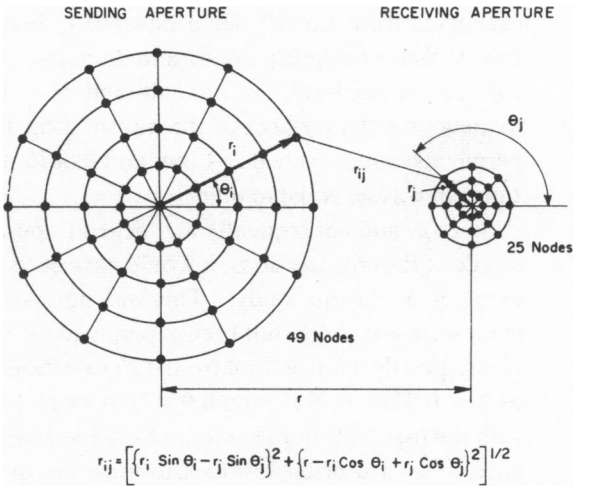

FIGURE 2

FIGURE 1 S-function (in arbitrary units) vs. μ for different distances between transmitting and receiving points.
FIGURE 2 Schematic representation of the node positions on the surface of the sending and receiving aperatures.

and receiving have finite areas, thus requiring the specification of transmitting and receiving functions.

The two functions selected were the constant step and chopped Gaussian functions. In the case of the step function, it was assumed that the transmitting optical fiber generated a constant beam of normal incident light across its transmitting surface and the receiving fiber was uniformly capable of receiving light across its surface. In the second case, Gaussian distributed transmission and reception functions were selected at discrete spatial positions r_i from

$$M(r_i) = (K/\sigma\sqrt{2\pi}) \exp(-r_i^2/2\sigma^2), \quad |r_i| < 4\sigma. \tag{13}$$

Here the radius of the fiber-optic transmitting or receiving surface was equal to 4σ, while K is the normalization constant.

To account for these two types of source/receiver functions, the mean current, $\overline{J_{OUT}(r)}$, was obtained from

$$\overline{J_{OUT}(r)} = \sum_{i=0}^{M} M_S(r_i) \sum_{j=0}^{N} M_R(r_j) J_{OUT}(r_{ij}), \tag{14}$$

where $M_S(r_i)$ is the source magnitude at location r_i, measured from the center of the source fiber optic, and $M_R(r_j)$ is the receiver magnitude at r_j, measured with re-

spect to the center of the receiving fiber optic. The $J_{OUT}(r_{ij})$ is the reflected current, calculated from Eq. 10, for a distance r_{ij} between the nodes at r_i and r_j, as shown in Fig. 2. When using Eq. 14, 49 and 25 points were used across the source and receiver surfaces, respectively, i.e. $M = 48$ and $N = 24$. These values were selected to adequately span the surfaces of the transmitting and receiving fiber optics used in the experiments, which were 0.254 mm and 0.0635 mm radius, respectively. In all calculations, μ_0 was set equal to unity.

Since $\bar{\mu}$, and consequently λ_{tr}, depend upon the shape of $\sigma_s(\mu)$, as well as the magnitude of the cross sections, it would have been preferable to use an experimentally determined λ_{tr} in this study. This was not possible, however, since detailed angular cross section data has not been experimentally determined for light scattering in blood. Consequently a range for $\bar{\mu}$ from 0.97 to 0.9950 was studied which bracketed the values of $\bar{\mu} = 0.9794$, 0.9913, and 0.9947, as extracted from the data (19) of the Appendix with the assumption that $\sigma_s(\mu)$ obeys the Henyey-Greenstein phase function (20), the purely-forward-or-backward scattering law, or Mie scattering, respectively.

In Fig. 3 the theoretical reflected current, from Eq. 14, for 0.685 μ wavelength light

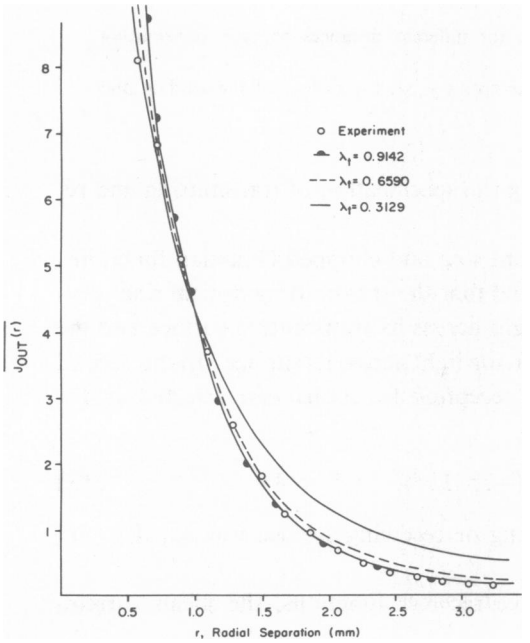

FIGURE 3

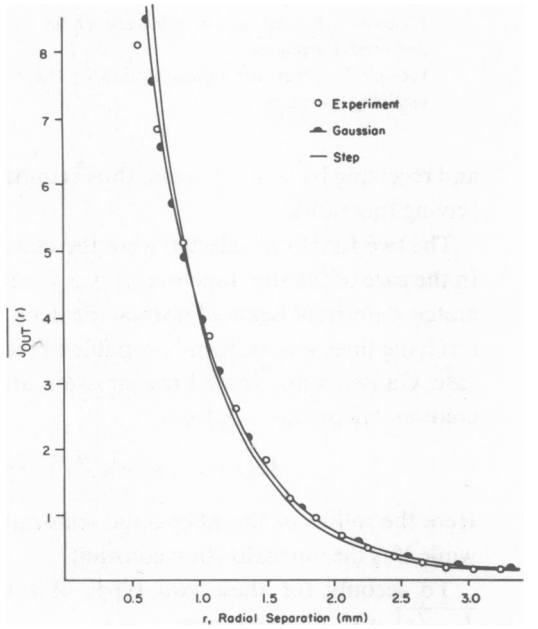

FIGURE 4

FIGURE 3 Reflected currents (in arbitrary units) vs. fiber center-to-center separation distance (in millimeters) for experimental measurements (19) of 0.685 μ light in 100% oxygen saturated blood and for theoretical calculations with different values of λ_{tr}.

FIGURE 4 Reflected currents (in arbitrary units) vs. fiber center-to-center separation distance (in millimeters) for experimental measurements (19) of 0.685 μ light in 100% oxygen saturated blood and for theoretical calculations with step and Gaussian functions.

is compared with reflectance from blood at 100% oxygen saturation and a hematocrit of $H = 0.41$ (19). The calculations for the reflected current are based on the Gaussian distributed source and receiver functions. The curves have been normalized at a center-to-center separation distance of 0.95 mm.

As can be seen, the calculated results agree best with experimental measurements for $\lambda_{tr} = 0.9142$ mm, corresponding to $\bar{\mu} = 0.9947$. A poorer comparison results from the use of $\lambda_{tr} = 0.6590$ and 0.3129 mm, corresponding to $\bar{\mu} = 0.9913$ and 0.9794, respectively.

In Fig. 4 the experimental results shown in Fig. 3 are compared with the reflected current for the Gaussian and step functions used for the source and receiver. It can be concluded from these curves that the calculations are relatively insensitive to the transmitting and receiving functions, but if anything the peaked, Gaussian distribution tends to be a better representation than the flat, step distribution.

As a last step in any theoretical analysis, it must be mentioned that in a fiber-optic catheter oximeter there is, of course, more than one fiber-optic for transmitting and one for receiving. The total reflected current, J_T, can be found for a complete fiber-optic bundle by summing the mean out-going currents at each receiving fiber for all sending fibers. The total reflected current is

$$J_T = \sum_{m=1}^{M} \sum_{n=1}^{N} \overline{J_{\text{OUT}}(r_{mn})} \tag{15}$$

for M transmitting optical fibers and N receiving fibers. The r_{mn} is the center-to-center distance of the mth sending and nth receiving optical fibers and $\overline{J_{\text{OUT}}(r_{mn})}$ is obtained from Eq. 14.

SUMMARY

An approximate expression for the reflected current has been numerically evaluated using angle-dependent transport theory and results for the reflectance from blood in the case of one transmitting and one receiving fiber optic were compared with experimental data. The comparison of the analytical results with values of the reflectance measured experimentally shows good agreement with Mie scattering data, and less so with the Henyey-Greenstein and purely-forward-or-backward models for scattering.

Calculations of the reflected current for constant step and chopped Gaussian transmission and reception functions, when compared with experimental results, showed that the actual transmitting and receiving functions seem to be more typical of the Gaussian shape which is peaked toward the center of the optical fibers. Furthermore, calculations of the reflected current for a range of the average cosine of the scattering angle indicated that the actual transport mean free path for 0.685 μ light in 100% oxygen saturated blood is about 0.9 mm. Finally, it may be concluded that there is a continuing need for more experimental research in the area of light scattering in blood. Specifically, there is no complete, detailed description of the scattering function, al-

though various researchers have obtained optical parameters applicable to diffusion or two-stream approximations for blood (9, 11, 12, 15).

Helpful comments from Dr. Peter Cheung of Case Western Reserve University were appreciated.

Received for publication 7 January 1974 and in revised form 1 August 1975.

APPENDIX: DATA FOR LIGHT SCATTERING IN BLOOD

For purposes of correlating analytical calculations with experimental measurements, we consider blood with a hematocrit of 0.41 and a hemoglobin content of normal blood. Then for 0.685 μ light, we take the experimental values of $\sigma_s^+ = 140.7$ mm^{-1} and $\sigma_s^- = 0.615$ mm^{-1}, with $\sigma_a = 0.265$ mm^{-1} for a hematocrit of $H = 0.41$ and 100% oxygen saturation (15). Here the forward and backward scattering cross sections, σ_s^+ and σ_s^-, respectively, are defined as

$$\sigma_s^+ = 2\pi\,\sigma_s \int_0^1 f(\mu)\,d\mu, \tag{16}$$

$$\sigma_s^- = 2\pi\,\sigma_s \int_{-1}^0 f(\mu)\,d\mu, \tag{17}$$

and σ_a is the absorption cross section. The relationship between the absorption and scattering cross sections with this data, for example, is consistent with Mie scattering calculations (15), done by approximating an erythrocyte as a sphere (21, 22). These cross sections provide information about the directional nature of the scattering and are basic parameters in the two-stream approach (23, 24) and diffusion theory. In this notation, the mean number of secondaries per collision is

$$w = (\sigma_s^+ + \sigma_s^-)/(\sigma_s^+ + \sigma_s^- + \sigma_a).$$

To describe the anisotropic scattering we may use the Henyey-Greenstein differential scattering function, which has one independent parameter g to be fit to the data (20),

$$f(\mu) = (4\pi)^{-1}(1 - g^2)(1 + g^2 - 2g\,\mu)^{-3/2}, \qquad -1 \le g \le 1. \tag{18}$$

Another possibility is to use the purely-forward-or-backward scattering law,

$$f(\mu) = (4\pi)^{-1}[\delta(\mu - 1) + \delta(\mu + 1)]. \tag{19}$$

Two other one-parameter models for $\sigma_s(\mu)$, the binominal and the ellipsoidal laws given by

$$f(\mu) = \pi^{-1}[(N + 1)/(2^{N+2})](1 + \mu)^N, \qquad N \text{ constant}, \tag{20}$$

and

$$f(\mu) = \frac{(b/2\pi)}{\ln[(1 + b)/(1 - b)]}(1 - b\,\mu)^{-1}, \qquad -1 < b < 1, \tag{21}$$

respectively, have been examined and are believed to be inferior to the function of Eq. 18 as one-parameter functions for light scattering in blood.

The average cosine of the scattering angle for the Henyey-Greenstein phase function is calculated from $\bar{\mu} = g$, where g is obtained from σ_s^+/σ_s^- as the solution of the equation

$$\frac{[(1 + g^2 - 2g)^{-1/2} - (1 + g^2)^{-1/2}]}{[(1 + g^2)^{-1/2} - (1 + g^2 + 2g)^{-1/2}]} = \frac{\sigma_s^+}{\sigma_s^-}. \tag{22}$$

For the model in which the scattering is purely forward or purely backward,

$$\bar{\mu} = (\sigma_s^+ - \sigma_s^-)/(\sigma_s^+ + \sigma_s^-). \tag{23}$$

Using the preceding experimental data gives $\bar{\mu} = 0.9794$ and 0.9913 for the Henyey-Greenstein and purely-forward-or-backward scattering laws, respectively, while the value of $\bar{\mu}$ from Mie scattering calculations is 0.9947.

REFERENCES

1. POLANYI, M., and R. HEHIR. 1962. In vivo oximeter with fast dynamic response. *Rev. Sci. Instrum.* **33**:1050.
2. ENSON, Y., W. BRISCOE, M. POLANYI, and A. COURRAND. 1962. In vivo studies with an intravascular and intracardiac reflection oximeter. *J. Appl. Physiol.* **17**:552.
3. MOOK, G., P. OSYPA, R. STURM, and E. WOOD. 1969. Fiber optic reflection photometry on blood. *Cardiovasc. Res.* **2**:199.
4. KAPANY, N., and N. SILBERTRUST. 1964. Fiber optics spectrophotometer for in vivo oximetry. *Nature (Lond.).* **204**:138.
5. LOWINGER, E., A. GORDON, A. WEINREB, and J. GROSS. 1962. Analysis of a micromethod for transmission oximetry of whole blood. *J. Appl. Physiol.* **19**:1179.
6. ANDERSON, N. M., and P. SEKELJ. 1967. Light-absorbing and scattering properties of nonhaemolysed blood. *Phys. Med. Biol.*, **12**:173.
7. TWERSKY, V. 1962. Multiple scattering of waves and optical phenomena. *J. Opt. Soc. Am.* **52**:145.
8. LONGINI, R., and R. ZDROJKOWSKI. 1968. A note on the theory of backscattering of light by living tissue. *IEEE Trans. Bio-Med. Eng.* **BME-15**:4.
9. ZDROJKOWSKI, R., and N. PISHAROTY. 1970. Optical transmission and reflection by blood. *IEEE Trans. Bio-Med. Eng.* **BME-17**:122.
10. JOHNSON, C. 1970. Optical diffusion in blood. *IEEE Trans. Bio-Med. Eng.* **BME-17**:129.
11. COHEN, A., and R. LONGINI. 1971. Theoretical determination of the blood's relative oxygen saturation in vivo. *Med. Biol. Eng.* **9**:61.
12. JANSSEN, F. 1972. A study of the absorption and scattering factors of light in whole blood. *Med. Biol. Eng.* **10**:231.
13. RYBICKI, G. 1971. The searchlight problem with isotropic scattering. *J. Quant. Spectrosc. Radiat. Transfer.* **11**:827.
14. BELL, G., and S. GLASSTONE. 1970. Nuclear Reactor Theory. Van Nostrand-Reinhold Co., New York. 105.
15. REYNOLDS, L., J. MOLCHO, C. JOHNSON, and A. ISHIMARU. 1974. Optical cross-sections of human erythrocytes. *Proc. 27th Annu. Conf. Eng. Med. Biol.* **16**:58.
16. CHANDRASEKHAR, S. 1950. Radiative Transfer. Oxford University Press, London.
17. HUMMER, D., and G. RYBICKI. 1967. Methods in Computational Physics. B. Alder, S. Fernbach, and M. Rotenberg, editors. Academic Press, New York. **7**:53.
18. COOLEY, J., P. LEWIS, and P. WELCH. 1967. Applications of the fast Fourier transform to computation of Fourier integrals, Fourier series, and convolution integrals. *IEEE Trans. Audio Electroacoustics.* **AU-15**:79.
19. REYNOLDS, L., C. JOHNSON, and A. ISHIMARU. 1974. Optical reflectance measurements made by a two fiber cuvette. *Proc. 27th Annu. Conf. Eng. Med. Biol.* **16**:308.
20. HENYEY, L., and J. GREENSTEIN. 1941. Diffuse radiation in the galaxy. *Astrophys. J.* **93**:70.
21. KREID, D., M. KAMMIN, and R. GOLDSTEIN. 1971. Measurements of light scattering characteristics of red cell, red cell "ghosts" and polystyrene spheres. *Proc. 24th Annu. Conf. Eng. Med. Biol.* **13**:143.
22. CHEUNG, P. 1973. Effects of blood physiological variations on optical scattering and fiberoptic oximetry. Ph.D. Thesis. Electrical Engineering Department, University of Washington, Seattle.
23. KUBELKA, P., and F. MUNK. 1931. Reflection characteristics of paints. *Z. Tech. Physik.* **12**:593.
24. KUBELKA, P. 1948. New contributions to the optics of intensely light-scattering materials. *J. Opt. Soc. Am.* **38**:448.